4th Conference on Sustainability in Civil Engineering (CSCE'22)
Department of Civil Engineering
Capital University of Science and Technology, Islamabad Pakistan

Numerical Study of Shape Memory Alloy (SMA) Reinforced Beam Subjected to Seismic Loading

[a] Juna Bloy, [b] Rabee Shamass, [c] Vireen Limbachiya, [d,e] Mohammed El-desoqi*

a: Civil and Building Services Engineering, London South Bank University, junabloy23@gmail.com
b: Civil and Building Services Engineering, London South Bank University, shamassr@lsbu.ac.uk
c: Civil and Building Services Engineering, London South Bank University, limbachv@lsbu.ac.uk
d: Civil Engineering Department, Faculty of Engineering, The British University in Egypt (BUE), El-Sherouk, Cairo, Egypt, mohammed.eldesoqi@bue.edu.eg
e: Civil and Building Services Engineering, London South Bank University, eldesoqm@lsbu.ac.uk
* Corresponding author: Email ID: shamassr@lsbu.ac.uk

Abstract- To safeguard against the loss of life and to maintain integrity, reinforced concrete structures are designed and constructed to withstand severe damage, impact and permanent displacement during a strong earthquake. Due to the dissipation of energy after a major earthquake, steel reinforcement undergoes large strains which lead to damage in the plastic hinge zone. Furthermore, the structure will be unserviceable due to the large residual deformations caused by the permanent strain in steel. Implementation and development of smart materials in structures will help to achieve these qualities. Shape Memory Alloy (SMA) is an example of a smart material, the use of such super elastic material in reinforced structures helps to recover the strain upon unloading which leads to improved recovery. without significant degradation or permanent deformation through repeated cycling. This ability gives a promise in civil engineering infrastructure applications specifically in seismic design. The primary objective of this study is to review the use of SMA in reinforced concrete at the plastic hinge region and to review the behavior of the hybrid beam using finite element software. After validation of the finite element model with the experimental results gathered from past literature, a parametrical study is conducted to understand the behavior of the hybrid beam with a change in parameters.

Keywords- Numerical study, RC beam, Shape Memory Alloy (SMAs), VecTor2

1. Introduction

When exposed to major earthquakes, ductile structures are built to respond inelastically. This is usually accomplished by placing plastic hinges at strategic spots throughout a building. The plastic hinges are engineered to provide flexure while avoiding nonductile failure mechanisms. While this prevents the structure from collapsing and ensures that the earthquake's energy is released effectively, residual deformations are to be expected. As the reaction continues into the inelastic region, residual deformation is mostly caused by the accumulation of residual strains in the reinforcement. After a seismic event, significant residual deformations can render structures unusable It may also make repair and retrofitting impossible. However, a comparatively new class of alloys called as Shape Memory Alloys (SMAs) has just developed and piqued researchers' interest. Shape memory alloys are one-of-a-kind materials that change the crystalline phase when exposed to temperature or stress changes, and they come in two varieties: Austenite and Martensite. Due to their capacity to recover inelastic displacements, these alloys are appealing in seismic applications. Furthermore, at significant stresses, SMAs yield under load and strain hardening and have the same strength capacity as traditional deformed reinforcing bars. The high initial cost of SMAs is one of their key disadvantages; as a result, they should only be employed in vital areas. Another drawback is the reduced capacity to disperse energy due to its re-centering tendencies. The higher crack widths and crack spacing that should be expected in concrete members reinforced with SMAs because of their smooth surface are envisaged to a lesser extent. SMAs, on the other hand, are corrosion resistant and can tolerate higher crack widths than typical deformed bars.

Various research studies have been worked upon to improve the seismic resistance of concrete structures by using SMAs in critical regions to reduce residual deformation [1]. To allow the dissipation of energy in the critical region and to allow yielding, and to recover deformation, SMAs were used in various RC structures such as beam-column joints [2], in beams [3], ~~and~~ in shear walls [4, 5], and in reinforced concrete (RC) columns [6]. They found that in the event of an earthquake, SMA enables the structure to recover its residual deformation after yielding. However, there have been few numerical investigations of hybrid steel-SMAs reinforced concrete beams. Therefore, the main purpose of the paper is to build a numerical model for hybrid steel-SMAs reinforced concrete beams and conduct a validation against the experimental results conducted by Abdulridha et al. [3] in terms of ultimate capacity and hysteresis behaviour. Finally, a parametric study is conducted to investigate the effect of various reinforcement ratios as well as the concrete compressive strength on the seismic behaviour of hybrid steel-SMAs reinforced beams.

2. Review of Experimental Results

Abdulridha et al. [3] tested seven simply supported concrete beams subjected to monotonic, cyclic, and reverse cyclic loading. Nickel-Titanium SMA (Nitinol) alloy is used in the experiment. The goal of this experimental program was to look at the structural behaviour of SMA-reinforced beams and assess their applicability to be used as an alternative to steel in seismic applications. In the numerical modelling conducted in this paper, only two beam tests, Beams B3-SR and B6-NR will be explored in depth, both were subjected to reverse cyclic loading. B3-SR and B6-NR are reinforced with conventional steel and hybrid steel-SMA rebars, respectively. For B3-SR, 10M (11.3mm diameter) steel bars were used. centre of B6-NR was reinforced with 12.5 mm diameter Superelastic SMA smooth bars and coupled to 15M steel rebars (16 mm) (Fig. 2). The beams were 2800 x 125 x 250 mm (2400 mm from centre to centre of supports). Two central point loads, typically spaced at 125 mm apart, were used to maintain a consistent flexural zone (critical section). The SMA bars were utilized for a total length of 600 mm, centred at the beams' midspan. The SMA bars were threaded at the ends and threaded mechanical couplers were used to link them to the steel rebars. To enhance yielding at the midspan and away from the threaded sections at the ends of the bars, the SMA bars were reshaped to a diameter of 9.5 mm over a 300 mm length. The couplers had a diameter of 12.6 mm and a length of 50 mm. The shear reinforcement, which consisted of closed stirrups with a diameter of 6.35 mm, was everywhere spaced at 100 mm along the length of the beam. A typical test specimen installed in the testing apparatus is seen in Figure 1. To prevent the concrete from being crushed, a steel plate (75x150x25mm) was installed below each point stress. A hydraulic jack with displacement control was used to apply the load. Load cells were employed to measure the applied forces, and displacement cable transducers were used to continually record deflection values at the midspan (DCTs). ATC-24 [~~5~~7], was used to apply reverse cyclic stress. Single repetitions at each displacement level were the sole change. One cycle of loading was performed at 0.33y, 0.66y, and 1.0y, where y is the yield displacement. Then, until failure, the following cycles were based on multiples of y. The yield displacement of the SMA and conventional reinforced beams was approximately 6.4 mm and 5.7 mm, respectively.

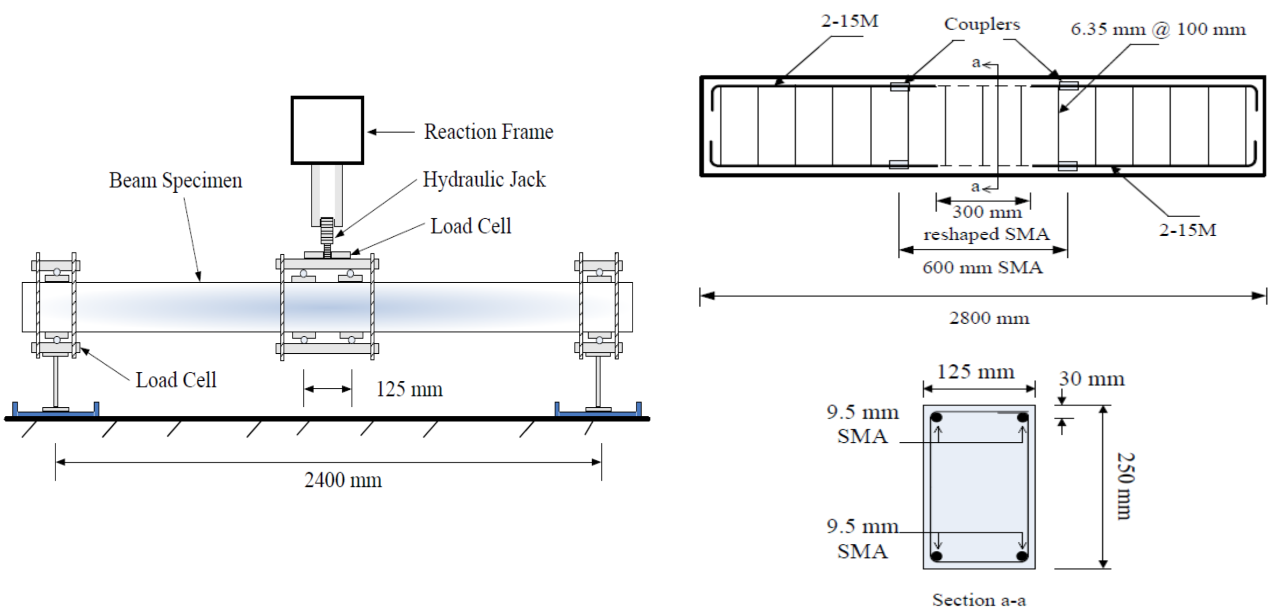

Figure 1. Typical test specimen and beam cross section

The SMA bars had a modulus of elasticity of around 60 GPa, whereas the 10M distorted bars had a modulus of elasticity of roughly 205 GPa. The approximate yield stress for the SMA was determined to be 415 MPa, somewhat lower than the 425 MPa and 440 MPa yield stresses for the 10M and 15M conventional steel, respectively, based on a 0.2% offset. At around 1.5% strain, the ordinary steel experienced strain hardening. Hardening of the SMA bar occurred at a strain of around 5%. The ultimate strength for 10M, 15M and SMA rebars was 615 MPa, 650 MPa and 800 MPa, respectively. Concrete of conventional strength with 10 mm aggregates size was used to build the beams. On the day of testing, the SMA and conventional reinforced beams had average compressive strengths of 32.7 MPa and 34.6 MPa, respectively.

3. Numerical modelling and validation

A preliminary model was created and implemented in the nonlinear two-dimensional finite element software VecTor2 (Ver.4.4) [~~6~~8], which is suitable for membrane structures. Based on the Modified Compression Field Theory and the Disturbed Stress Field Model, VecTor2 utilizes a smeared, rotating-crack formulation [9~~7~~]. Both conventional and SMA beams were modelled, and the results were compared with the test results. All beams were modelled with rectangular plane stress concrete elements. The longitudinal flexural reinforcement bars were modelled with discrete truss bar elements and the transverse shear reinforcement was modelled with smeared within the concrete elements. For modelling conventional steel reinforcement, the truss bars were assumed perfectly bonded to the surrounding concrete while the SMA bars were partially bonded given the smooth surface of the bars leading to lower bond stresses. The applied load followed the same loading protocol in the test. The finite element model for the beams B3-SR and B6-NR are as shown in Figure 2. To coincide with the node of the concrete rectangular elements, the length of each truss element was 25 mm. Bond-slip elements were used to represent the bond between the SMA bars and the concrete, and it was assumed that the typical deformed reinforcement and couplers in SMA beams were perfectly connected to the surrounding concrete. Prior to the slippage, the bond-slip components were specified by paired nodes with the same coordinate. A concrete element was attached to one of the nodes, while a discrete reinforcement element was added to the other. At one end of the beam, pins were used to represent the supports, which were simulated with vertical and horizontal restraints, while at the other end, rollers were used to represent the supports, which were only provided with vertical restraints. The restraints were only attached at one end throughout the analysis, which was sufficient to simulate the behaviour of the supports.
Using two loading plates, two vertical loads spaced 125 mm apart were applied uniformly at mid-span in the experimental setup. In the Finite Element Model, each applied load at the top of the beam were represented by four nodes. That means four nodes were assigned at the top of the beam to apply the loads. To prevent the local crushing of the concrete the distributed load was intended to represent the spreading of the load due to the loading plate.
The reinforcement, concrete and bond constative models are illustrated in Table 1. The detailed descriptions of each model were described in the Vector2 Manual. Typically, the default models are chosen unless an alternative model better captures the behavioural response.

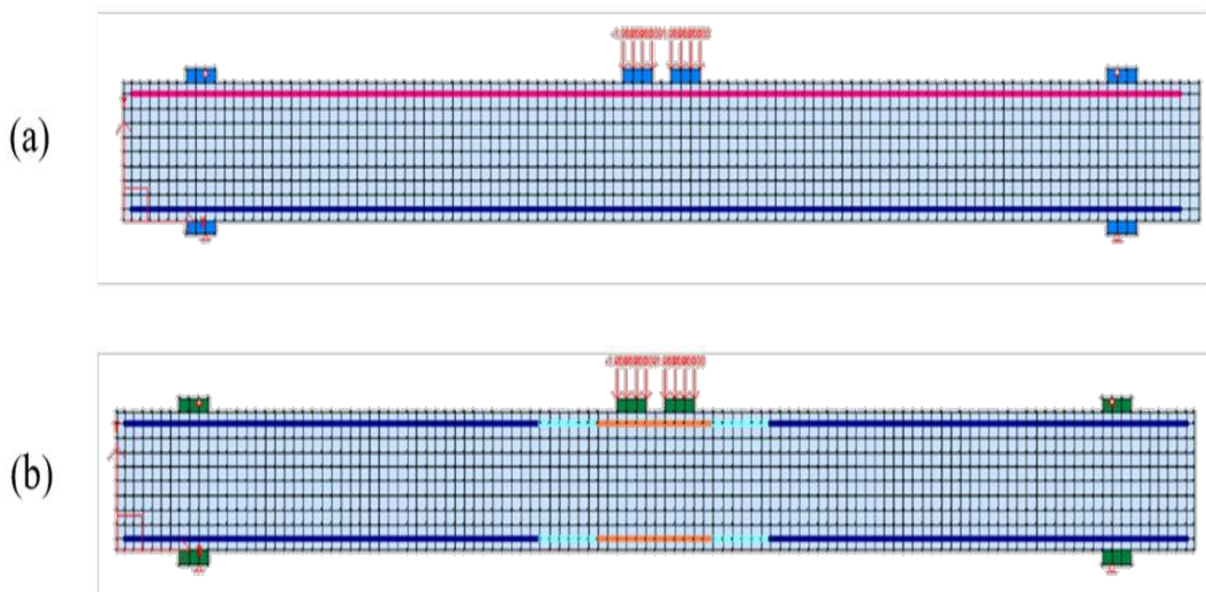

Figure 2: Finite element model of beam (a) B3-SR and (b) B6-NR

Table 1 Material and Behavioural models

Material Property	Material Model
Concrete Compression Base Curve	Popovics (NSC)*
Compression Post-Peak	Base Curve*
Concrete Compression Softening	Vecchio 1992-A
Concrete Tension Stiffening	Modified Bentz
Concrete Tension Softening	Linear
Concrete Tension Splitting	Not Considered
Concrete Confinement Strength	Kupfer I Richart
Concrete Dilatation	Variable - Kupfer
Concrete Cracking Criterion	Mohr-Coulomb (Stress)
Concrete Crack Width	Agg/5 Max Crack Width
Concrete Hysteresis	Non-Linear with Plastic Offset
Slip Distortion	Vecchio-Lai
Reinforcement Hysteretic Response	Seckin Model (Bauschinger)
Reinforcement Dowel Action	Tassios Model (Crack Slip)
Reinforcement Buckling	Asatsu Model
Concrete Bond	Eligehausen Model

4. Numerical validation

The responses of the conventional reinforced and SMA reinforced beams are shown in Figures 3 (a) and (b), respectively. The strength capacities are often effectively replicated and match the experimental tests. The nonlinear unloading response of the SMA reinforced beam found during testing suggests that the recovery is significantly overstated, and the unloading curves do not represent the nonlinear unloading response of the SMA reinforced beam. The analytical response of a conventional reinforced beam is shown in Figure 3 (b) for comparison. The behaviour seen during testing, including strength and ductility capabilities, was successfully represented by the numerical model. Unloading and reloading curves were accurately modelled. The pinching is a noteworthy difference; slightly more was noted during testing. With a modified constitutive model for SMA bars that reflect nonlinear unloading and minor residual stresses accumulated as the ductility needs grow, better results for the SMA beam may be produced. Because reverse cyclic loading involves loading and unloading the beam in one cycle, the unloading and reloading curves following reverse cyclic loading were accurately modelled. In the analysis of the conventional beam, the analysis predicted slightly lower strength and higher initial stiffness than the experimental results. The measured displacement at failure following the numerical test was 57.125mm, however, the expected displacement was 59 mm. There were also differences that were noted around the yield strength. The observed value was 29 kN for the experimental test, however, the analysis revealed a value of 26.19 kN which is less than the experimental value of almost 9.7%. Both beams failed by concrete crushing after significant yielding of the longitudinal reinforcement but at slightly different displacements. In general, though, the numerical response of the conventional reinforced beam demonstrates the applicability of the finite element model and VecTor2 adopted for this study.

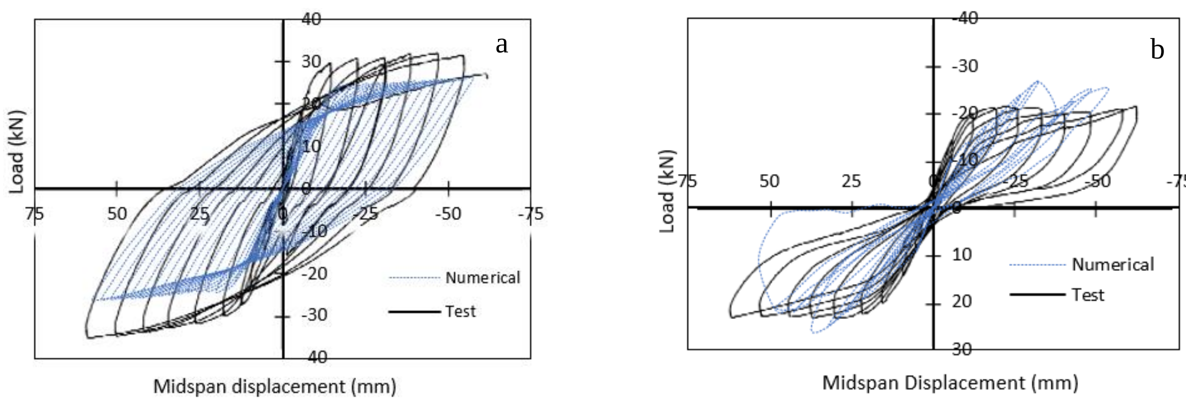

Figure 3: Analytical load-displacement response of beam (a) B3-SR and (b) B6-NR

The calculated response of the SMA reinforced beams indicates that the analysis reasonably predicted the behavior observed during testing. Comparing the observed results to the predicted numerical results, the predicted ultimate strength of B6-NR was 24.5 kN, however, the observed and recorded values for the experimental load capacity was 21.94 kN which is less than the predicted value of 10.45%. The difference in the value of ultimate load capacity is due to a large fracture outside the critical zone that occurred during the test procedure on this SMA beam. The midspan displacement at failure measured by the experiment was 60 mm, while the numerical analysis yielded a value of 53.29 mm. Permanent displacements were satisfactorily captured during the analysis; however, more pinching was observed in the experimental hysteretic response. Figure 3 (b) demonstrates the hysteretic behavior was well simulated, including peak strength, ductility, residual displacements, and unloading response. The discrepancy in the ultimate load capacity can be attributed to the fact that the SMA beam experienced a major crack outside the critical region during the test which resulted in a reduction in strength.

By comparing the computed and actual cracking patterns, the numerical models were further evaluated. As demonstrated in Figure 4, the model predicted closely spaced cracks in the conventional reinforced beam and much wider cracks in the SMA reinforced beam. These patterns matched observations made during testing, indicating that the finite element model was correct. These trends were consistent with observations noted during testing. Generally, the finite element results provided good predictions of the sequence and locations of the first flexural and shear cracks. For comparison purposes, the first numerical crack was defined by a crack width of 0.10 mm, which corresponds to the visible crack width during testing. Experimentally, flexural cracking at midspan was observed first followed by inclined shear cracks near the supports. Numerically, the sequence of cracking was similar to that observed in the conventional and SMA beams where local effects from the presence of the couplers governed the location of critical damage. This resulted in the first flexural crack initiating at the coupler location where failure was observed. All beams were designed as flexural members that experience significant reinforcement yielding prior to concrete crushing. This type of failure was predicted in the finite element analysis for both conventional and SMA beams. Experimentally, the tested beams had similar failure modes except for SMA beam which experienced failure by rupturing of the SMA at the transition point where the SMA changed diameter.

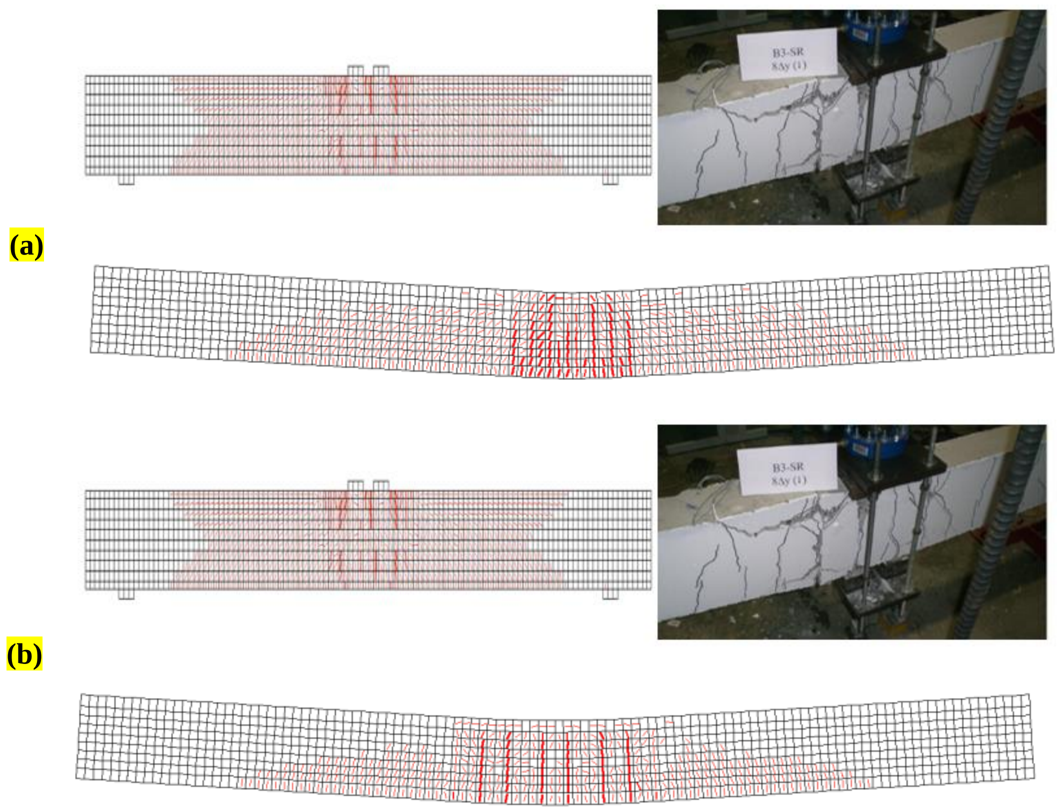

Figure 4: Crack Patterns of beam (a) B3-SR and (b) B6-NR

5. Parametric study

This part includes the changes in the seismic behaviour of Superelastic SMAs caused by varying the concrete strength and SMA reinforcement ratio of the beam B6-NR validated in the previous section. By using different SMA rebar diameter, SMA reinforcement ratio has been modified to get the reinforcement ratios of 0.20 %, 0.50 %, 0.80 %, and 1.07 %. In the second parametric study, the compressive strength of concrete is varied such as 30, 40, 50, and 60 MPa. Figure 5(a) and (b) show the effect of the reinforcement ration of the SMA on the envelop load-deflection curves and cumulative energy dissipation curves, respectively. It can be noted that as the reinforcement ratio increase, the ultimate load-carrying capacity slightly increases which allow the beam to sustain the more applied load. For instance, as the reinforcement ratio increases from 0.2% to 0.8%, the ultimate load capacity increases by 26% this is due to the beam becoming more ductile to sustain the extra applied load. Furthermore, an increase in the reinforcement ratio results in improvements in energy dissipation due to an increase in the overall ductility of the wall which leads to an increase in the area under the response curve. As the reinforcement ratio increases, the load-carrying capacity and the strength of the beam also increase so that the amount of energy dissipated will also increase.

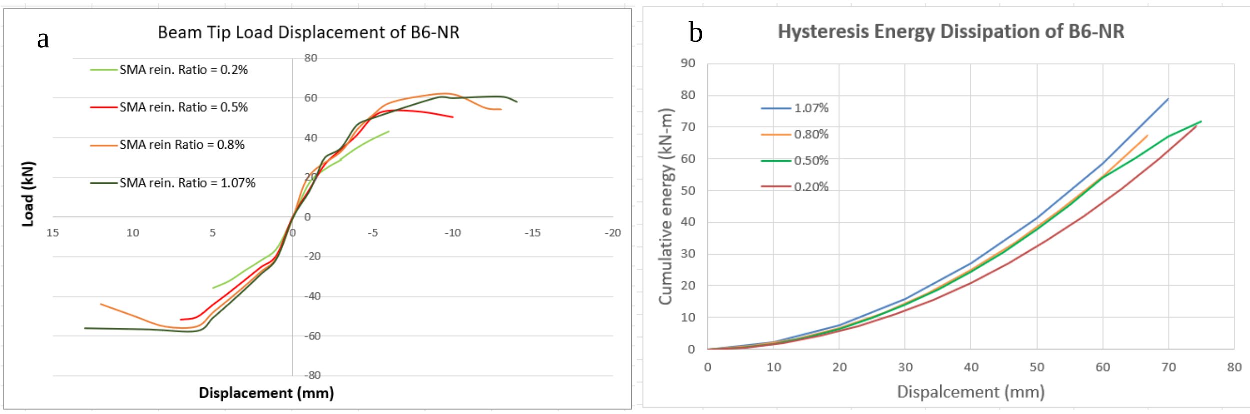

Figure 5:(a) Comparison of envelopes of load-displacement curves for SMA reinforcement ratio (b) Comparison of cumulative energy dissipation curves for SMA reinforcement ratio

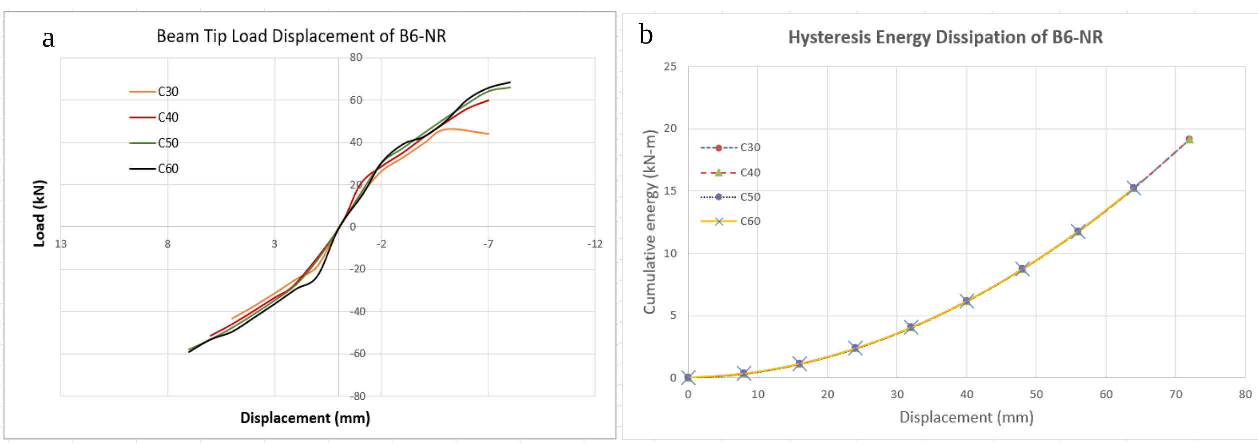

Figure 6:(a) Comparison of envelopes of load-displacement curves for concrete grades (b) Comparison of cumulative energy dissipation curves for concrete grades

When comparing the impact of concrete grades (C30, C40, C50 and C60), the ultimate load carrying capacity is increasing with an increase in the concrete grade, but all models failed in the last cycle. For example, as the compressive strength increase from 30MPa to 60MPa, the ultimate load capacity increase by 55%. There is only a marginal increase that can be found in the energy dissipation graph. Figure 9 shows the comparison results of load-displacement curves of various concrete grades.

6. Research significance

Long-term reverse cycle loads can cause fatigue failure in concrete flexural components reinforced with conventional steel, even at loads below their ultimate capacity. The goal of the current study project was to analyse the behaviour of concrete beams reinforced with a mix of conventional steel and SMA to reduce the risk of fatigue failure. Due to their superelasticity and high yield strength characteristics, SMAs may dissipate strain energy and recover deflection when used as reinforcement in RC flexural components. The findings of this study will help scientists and engineers better understand how concrete flexural components behave when reinforced with SMA and steel.

7. Conclusion

Based on the results, the following conclusions can be drawn:

- Nitinol SMA outperformed conventional beams in terms of minimizing residual movement in concrete beams and SMA reinforced beams have lower stiffness than conventional beams.
- The proposed numerical model using Vector2 provides accurate predictions in comparison with the test results for both conventional and hybrid steel-SMA rebars.
- In the case of parametric analysis with changing reinforcement ratios and concrete grade, the stress-strain behaviour and energy dissipation improve dramatically as the value of the parameters increases.
- The bigger diameter of Nitinol bars will assist in dissipating more energy and perform better in seismically active areas, but it is much more expensive than the smaller diameter, making it practically unfeasible in some circumstances.
- Finally, the ability to recover inelastic deformations, display strain hardening, and exhibit yielding while maintaining significant displacement ductility make Super-elastic SMA a promising alternative reinforcement in seismic design.
- However, because of the high initial cost, SMA may only be used in RC structures to a limited extent. As a result, in the design of reinforced members, optimization is essential.

References

[1] Saiidi, M.S. and Wang, H., 2006. Exploratory study of seismic response of concrete columns with shape memory alloys reinforcement. ACI Materials Journal, 103(3), p.436.

[2] Youssef, M., M. Alam, and M. Nehdi, 2008. Experimental investigation on the seismic behaviour of beam-column joints reinforced with superelastic shape memory alloys," Journal of Earthquake Engineering, 12, 1205-1222.

[3] Abdulridha, A., Palermo, D., Foo, S. and Vecchio, F. J. (2013) Behavior and modeling of superelastic shape memory alloy reinforced concrete beams, Engineering Structures, 49, pp. 893–904. DOI: 10.1016/j.engstruct.2012.12.041.

[4] Abdulridha, A. and Palermo, D., 2017. Behaviour and modelling of hybrid SMA-steel reinforced concrete slender shear wall. Engineering Structures, 147, pp.77-89.

[5] Hoult, R.D. and de Almeida, J.P., 2022. Residual displacements of reinforced concrete walls detailed with conventional steel and shape memory alloy rebars. Engineering Structures, 256, p.114002.

[6] Lee, C.S., Choi, E. and Jeon, J.S., 2022. Estimating the plastic hinge length of rectangular concrete columns reinforced with NiTi superelastic shape memory alloys. Engineering Structures, 252, p.113641.

[~~5~~7] ATC-24, 1992. Guidelines for Cyclic Seismic Testing of Components of Steel Structures, Applied Technology Council, Redwood City, CA.

[~~6~~8] Wong, P.S., and F. J., Vecchio, 2002. VecTor2 & Formworks user's manual, University of Toronto, Toronto, Canada.

[~~7~~9] Vecchio, F. J., 2000. Disturbed stress field model for reinforced concrete: formulation, Journal of Structural Engineering, ASCE, 126(9), 1070-1077.